

Syntheses, structures, fluorescent properties and natural bond orbital analyses of metal–organic complexes based on 5,6-substituted 1,10-phenanthroline derivatives



Lei Wang^a, Liang Ni^{a,*}, Jia Yao^b

^aSchool of Chemistry and Chemical Engineering, Jiangsu University, Zhenjiang 212013, People's Republic of China

^bDepartment of Chemistry, Zhejiang University, Hangzhou 310027, People's Republic of China

ARTICLE INFO

Article history:

Received 26 February 2013

Accepted 29 April 2013

Available online 9 May 2013

Keywords:

Metal–organic complex

Fluorescent property

NBO analysis

Structural diversity

ABSTRACT

Six new metal–organic coordination complexes, $[\text{Cd}(\text{MEDPQ})(2,5\text{-pydc})]_n$ (**1**), $[\text{Cd}_2(\text{MOPIP})_2(2,5\text{-pydc})_2]_n$ (**2**), $[\text{Cu}_2(\text{MOPIP})_2(2,5\text{-pydc})_2] \cdot \text{H}_2\text{O}$ (**3**), $[\text{Mn}(\text{MOPIP})_2(2,5\text{-pydc})] \cdot 3\text{H}_2\text{O}$ (**4**), $[\text{Cd}(\text{MOPIP})_2(2,6\text{-pydc})] \cdot 3\text{H}_2\text{O}$ (**5**) and $[\text{Cd}_2(\text{MOPIP})_2(2,3\text{-pydc})_2] \cdot \text{H}_2\text{O}$ (**6**) (MEDPQ = 2-methyldipyrido[3,2-f:2',3'-h]quinoxaline, MOPIP = 2-(4-methoxyphenyl)-1H-imidazo[4,5-f][1,10]phenanthroline, 2,5-H₂pydc = pyridine-2,5-dicarboxylic acid, 2,6-H₂pydc = pyridine-2,6-dicarboxylic acid, and 2,3-H₂pydc = pyridine-2,3-dicarboxylic acid), have been prepared through hydrothermal reactions. The transformation of coordination modes of transition metal ions and organic carboxylate ligands has a crucial influence on the multinuclear structures of these series. In compounds **1** and **2**, binuclear Cd(II) subunits occur, which are connected by 2,5-pydc anions to construct an undulating network. By selecting the different transition metal ions, we get the compounds **3** and **4**. For the compound **3**, the Cu(II) centers are linked by 2,5-pydc ligands to form a binuclear dimer. Compound **4** shows a mononuclear compound. For complexes **5** and **6**, by changing the dicarboxylate ligands, Cd(II) adopts a heptacoordinated mode to form a mononuclear compound and chain framework. In addition, fluorescent properties of **2–4** have been reported.

© 2013 Elsevier Ltd. All rights reserved.

1. Introduction

The development of new materials based on transition-metal ions and organic ligands, especially coordination polymers, has been greatly developed in the past decades. These coordination polymers can be rationally synthesized and tuned by a suitable choice of metal centers and organic ligands to control their framework structure and functionality [1]. Many metal complexes of 1,10-phenanthroline (1,10-phen) and its derivatives often show fascinating chemical and physical properties in the area of coordination chemistry, analytical chemistry, material chemistry, metalloenzymes, probes of nucleic acids, and redox processes, because of their fine π -conjugated character and strong chelating abilities [2,3]. Up to now, many kinds of 5,6-substituted 1,10-phen derivatives have been used as terminal or bridging ligands to prepare metal complexes [4–8]. In our paper, we chose two 5,6-substituted 1,10-phen derivatives 2-methyldipyrido[3,2-f:2',3'-h]quinoxaline and 2-(4-methoxyphenyl)-1H-imidazo[4,5-f][1,10]-phenanthroline (Scheme 1). Compared with 1,10-phen, an extended π -system of the two ligands contain potential supramolecular interactions for molecular recognition or assembly processes.

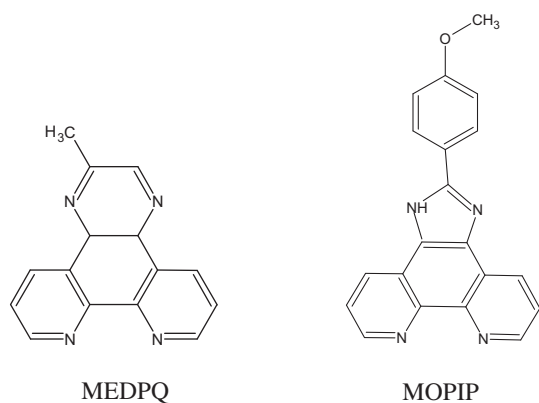
On the other hand, the rigid multicarboxylate-containing ligands with aromatic rings have been used to control, and adjust the topologies of these transition metal complexes. Compared with other dicarboxylic acids, the pyridine dicarboxylic acids have five donor atoms and it mainly coordinates to metal ion via the nitrogen and oxygen atom of carboxyl group, acting as a bridging linker [9]. Thus, the pyridine dicarboxylic acids may connect metal ions in different directions, generating multidimensional architectures.

As metal ions, Cd, Cu and Mn, with different radius, electronic properties and flexible coordination environment, exhibits variable coordination number and geometry with ligands [10], which inspire chemists' extensive interests in their fluorescence, magnetic and biological activities [11]. Thus, we tried to study the influence of transition metal coordination nature on the assembly of multinuclear subunits in compounds.

Herein, we report six new compounds with multinuclear structures, $[\text{Cd}(\text{MEDPQ})(2,5\text{-pydc})]_n$ (**1**), $[\text{Cd}_2(\text{MOPIP})_2(2,5\text{-pydc})_2]_n$ (**2**), $[\text{Cu}_2(\text{MOPIP})_2(2,5\text{-pydc})_2] \cdot \text{H}_2\text{O}$ (**3**), $[\text{Mn}(\text{MOPIP})_2(2,5\text{-pydc})] \cdot 3\text{H}_2\text{O}$ (**4**), $[\text{Cd}(\text{MOPIP})_2(2,6\text{-pydc})] \cdot 3\text{H}_2\text{O}$ (**5**) and $[\text{Cd}_2(\text{MOPIP})_2(2,3\text{-pydc})_2] \cdot \text{H}_2\text{O}$ (**6**) (MEDPQ = 2-methyldipyrido[3,2-f:2',3'-h]quinoxaline, MOPIP = 2-(4-methoxyphenyl)-1H-imidazo[4,5-f][1,10]phenanthroline, 2,5-H₂pydc = pyridine-2,5-dicarboxylic acid, 2,6-H₂pydc = pyridine-2,6-dicarboxylic acid, and 2,3-H₂pydc = pyridine-2,3-dicarboxylic acid). The influence of 5,6-substituted 1,10-phen

* Corresponding author. Tel.: +86 51188791800.

E-mail address: niliang@ujs.edu.cn (L. Ni).



Scheme 1. Structures of the MEDPQ and MOPIP ligands used in this work.

derivative, the coordination nature of transition-metal ions and the organic carboxylate linkers on the assembly of multinuclear subunits is discussed.

2. Experimental

2.1. General materials and methods

The neutral chelating ligands MEDPQ and MOPIP were synthesized according to the previous literature method [12]. Other reagents and solvents for synthesis were purchased from commercial sources and used as received. Transmission mode FT-IR spectra were obtained as KBr pellets between 400 and 4000 cm^{-1} using a Nicolet Nexus 470 infrared spectrometer. Elemental analysis was carried out with a Perkin-Elmer 240C analyzer. Thermogravimetric analysis (TG) was performed on a Germany Netzsch STA449C at a heating rate of 10 $^{\circ}\text{C} \cdot \text{min}^{-1}$ in nitrogen. Fluorescence measurement was carried out at room temperature with a Cary Eclipse spectrometer.

2.2. Computational procedures

All computations were performed using GAUSSIAN 03 program package [13] for complexes 2–4. The molecular structures for the

calculation were all from the initial X-ray structures of the complexes, which were used for the geometry optimization. All the subsequent calculations were performed based on the optimized geometries. Natural bond orbital (NBO) analyses were performed by applying 6-31+G(d) basis set for C, H, O, N atoms, and the effective core potential basis set Lanl2dz for metal atoms.

The molecular orbitals of 2–4 were plotted using the GAUSSIAN 03 view program.

2.3. Synthesis of the complexes 1–6

$[\text{Cd}(\text{MEDPQ})(2,5\text{-pydc})]_n$ (**1**): A mixture of $\text{Cd}(\text{OAc})_2 \cdot 2\text{H}_2\text{O}$ (0.133 g, 0.5 mmol), 2,5- H_2pydc (0.083 g, 0.5 mmol), MEDPQ (0.124 g, 0.5 mmol), NaOH (0.004 g, 0.1 mmol) and H_2O (18 mL) was placed in a 25 mL Teflon-lined stainless steel vessel under autogenous pressure at 165 $^{\circ}\text{C}$ for 5 days. After cooling to room temperature, red block crystals of **1** were collected by filtration and washed with distilled water in 60% yield (based on Cd). *Anal.* Calc. for $\text{C}_{22}\text{H}_{13}\text{N}_5\text{O}_4\text{Cd}$ (**1**): C, 50.45; H, 2.50; N, 13.37. Found: C, 50.47; H, 2.51; N, 13.35%. IR (KBr): $\nu = 3439$ (m), 3053 (m), 1628 (s), 1521 (m), 1474 (m), 1383 (s), 1334 (s), 1275 (m), 1167 (m), 1035 (w), 825 (m), 763 (m), 551 (w), 440 (w) cm^{-1} .

$[\text{Cd}_2(\text{MOPIP})_2(2,5\text{-pydc})_2]_n$ (**2**): Complex **2** was also synthesized by using a method similar to that described for the synthesis of **1** except that MOPIP (0.163 g, 0.5 mmol) was used instead of MEDPQ (0.124 g, 0.5 mmol). Yellow block crystals of **2** were collected by filtration and washed with distilled water in 52% yield (based on Cd). *Anal.* Calc. for $\text{C}_{54}\text{H}_{34}\text{N}_{10}\text{O}_{10}\text{Cd}_2$ (**2**): C, 53.70; H, 2.84; N, 11.60. Found: C, 53.71; H, 2.82; N, 11.62%. IR (KBr): $\nu = 3422$ (m), 3192 (m), 1612 (s), 1524 (m), 1482 (s), 1455 (m), 1386 (s), 1342 (s), 1255 (s), 1180 (m), 1074 (m), 822 (m), 769 (s), 509 (w), 477 (w) cm^{-1} .

$[\text{Cu}_2(\text{MOPIP})_2(2,5\text{-pydc})_2] \cdot \text{H}_2\text{O}$ (**3**): Complex **3** was also synthesized by using a method similar to that described for the synthesis of **2** except that $\text{Cu}(\text{OAc})_2 \cdot \text{H}_2\text{O}$ (0.1 g, 0.5 mmol) was used instead of $\text{Cd}(\text{OAc})_2 \cdot 2\text{H}_2\text{O}$ (0.133 g, 0.5 mmol). Green block crystals of **3** were collected by filtration and washed with distilled water in 78% yield (based on Cu). *Anal.* Calc. for $\text{C}_{54}\text{H}_{36}\text{N}_{10}\text{O}_{11}\text{Cu}_2$ (**3**): C, 57.50; H, 3.22; N, 12.42. Found: C, 57.52; H, 3.20; N, 12.41%. IR (KBr): $\nu = 3438$ (m), 3064 (m), 1611 (s), 1522 (s), 1482 (s), 1456 (s), 1344 (s), 1252 (m), 1182 (m), 1079 (m), 819 (m), 769 (s), 507 (w), 473 (w) cm^{-1} .

Table 1
Crystal data and structure refinements for compounds 1–6.

Parameters	1	2	3	4	5	6
Empirical formula	$\text{C}_{22}\text{H}_{13}\text{N}_5\text{O}_4\text{Cd}$	$\text{C}_{54}\text{H}_{34}\text{N}_{10}\text{O}_{10}\text{Cd}_2$	$\text{C}_{54}\text{H}_{36}\text{N}_{10}\text{O}_{11}\text{Cu}_2$	$\text{C}_{47}\text{H}_{33}\text{N}_9\text{O}_8\text{Mn}$	$\text{C}_{47}\text{H}_{31}\text{N}_9\text{O}_9\text{Cd}$	$\text{C}_{54}\text{H}_{34}\text{N}_{10}\text{O}_{11}\text{Cd}_2$
Formula weight (g mol^{-1})	523.78	1207.73	1128.03	906.76	978.22	1223.73
Crystal system	monoclinic	triclinic	triclinic	monoclinic	monoclinic	triclinic
Space group	$P2_1/c$	$P\bar{1}$	$P\bar{1}$	$P2_1/c$	$P2_1/c$	$P\bar{1}$
<i>a</i> (Å)	11.142(2)	9.4713(19)	8.6466(17)	10.8045(7)	17.442(3)	12.189(2)
<i>b</i> (Å)	10.256(2)	12.967(3)	10.411(2)	17.8202(12)	14.925(3)	13.987(3)
<i>c</i> (Å)	18.895(6)	19.570(4)	13.278(3)	21.5161(14)	17.640 (3)	14.323(3)
α ($^{\circ}$)	90	89.69(3)	106.84(3)	90	90	88.28(3)
β ($^{\circ}$)	111.17(3)	89.95(3)	102.57(3)	97.638(1)	114.36(3)	86.95(3)
γ ($^{\circ}$)	90	71.40(3)	95.93(3)	90	90	74.87(3)
<i>V</i> (Å ³)	2013.5(8)	2277.9(8)	1098.8(4)	4105.9(5)	4183.3(13)	2353.6(8)
<i>Z</i>	4	2	1	4	4	2
<i>D</i> _{calc} (g cm^{-3})	1.728	1.761	1.705	1.467	1.553	1.727
<i>F</i> (000)	1040	1208	576	1868	1984	1224
Absorption coefficient (mm^{-1})	1.126	1.012	1.052	0.391	0.594	0.982
<i>R</i> _{int}	0.0201	0.0266	0.0356	0.0492	0.0290	0.1154
Goodness-of-fit (GOF) on <i>F</i> ²	1.148	1.026	1.052	1.081	1.060	1.066
<i>R</i> ₁ ^a [<i>I</i> > 2 σ (<i>I</i>)]	0.0474	0.0335	0.0514	0.0619	0.0395	0.1154
<i>wR</i> ₂ ^b [<i>I</i> > 2 σ (<i>I</i>)]	0.1077	0.0715	0.1156	0.1785	0.0862	0.3315

^a $R_1 = \sum ||F_o| - |F_c|| / \sum |F_o|$.

^b $wR_2 = \{ \sum w(|F_o|^2 - |F_c|^2)^2 / \sum w(|F_o|^2)^2 \}^{1/2}$.

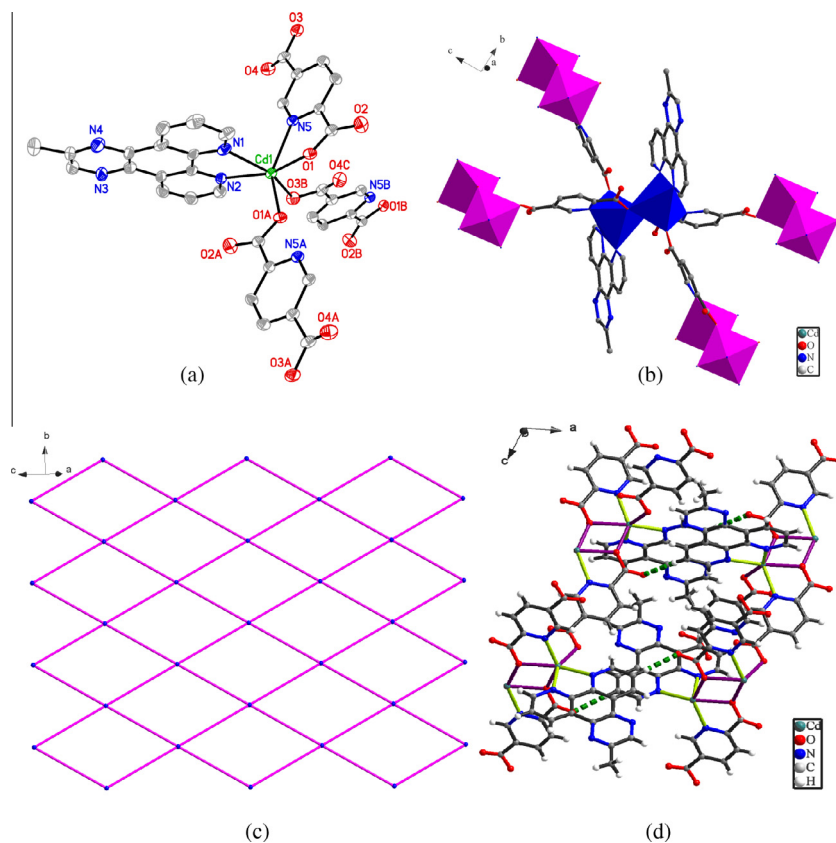


Fig. 1. (a) View of the coordination environment of Cd(II) in complex **1**; thermal ellipsoids are drawn at the 30% probability level. Hydrogen atoms have been omitted for clarity. (b) View of the linkage of the dinuclear core with four adjacent cores (H atoms and part of the aromatic rings are omitted for clarity). (c) The four-connected rhombic grid network of **1** along *bc* plan. (d) The supramolecular architecture by hydrogen bonding interactions (green broken lines represent hydrogen bonding interactions). (Color online.)

$[Mn(MOPIP)_2(2,5\text{-pydc})]\cdot 3H_2O$ (**4**): Complex **4** was also synthesized by using a method similar to that described for the synthesis of **2** except that $MnCl_2\cdot 4H_2O$ (0.099 g, 0.5 mmol) was used instead of $Cd(OAc)_2\cdot 2H_2O$ (0.133 g, 0.5 mmol). Yellow block crystals of **4** were collected by filtration and washed with distilled water in 55% yield (based on Mn). *Anal. Calc.* for $C_{47}H_{33}N_9O_8Mn$ (**4**): C, 62.19; H, 3.78; N, 13.89. Found: C, 62.21; H, 3.77; N, 13.88%. IR (KBr): $\nu = 3421$ (m), 3072 (m), 1609 (s), 1524 (s), 1482 (s), 1354 (s), 1254 (m), 1179 (m), 1076 (m), 836 (m), 738 (s), 514 (w), 478 (w) cm^{-1} .

$[Cd(MOPIP)_2(2,6\text{-pydc})]\cdot 3H_2O$ (**5**): Complex **5** was also synthesized by using a method similar to that described for the synthesis of **2** except that 2,6- H_2 pydc was used instead of 2,5- H_2 pydc. Yellow block crystals of **5** were collected by filtration and washed with distilled water in 62% yield (based on Cd). *Anal. Calc.* for $C_{47}H_{31}N_9O_9Cd$ (**5**): C, 57.71; H, 3.19; N, 12.89. Found: C, 57.73; H, 3.18; N, 12.86%. IR (KBr): $\nu = 3419$ (m), 3088 (m), 1614 (s), 1525 (m), 1485 (s), 1456 (m), 1427 (s), 1360 (s), 1256 (s), 1178 (m), 1075 (m), 841 (m), 734 (s), 512 (w), 480 (w) cm^{-1} .

$[Cd_2(MOPIP)_2(2,3\text{-pydc})_2\cdot H_2O]_n$ (**6**): Complex **6** was also synthesized by using a method similar to that described for the synthesis of **2** except that 2,3- H_2 pydc was used instead of 2,5- H_2 pydc. Yellow block crystals of **6** were collected by filtration and washed with distilled water in 68% yield (based on Cd). *Anal. Calc.* for $C_{54}H_{34}N_{10}O_{11}Cd_2$ (**6**): C, 53.00; H, 2.80; N, 11.45. Found: C, 53.01; H, 2.78; N, 11.46%. IR (KBr): $\nu = 3440$ (m), 3093 (m), 1607 (s), 1524 (m), 1482 (s), 1454 (m), 1398 (s), 1358 (s), 1251 (s), 1185 (m), 1073 (m), 831 (m), 740 (s), 534 (w), 448 (w) cm^{-1} .

2.4. X-ray crystallography

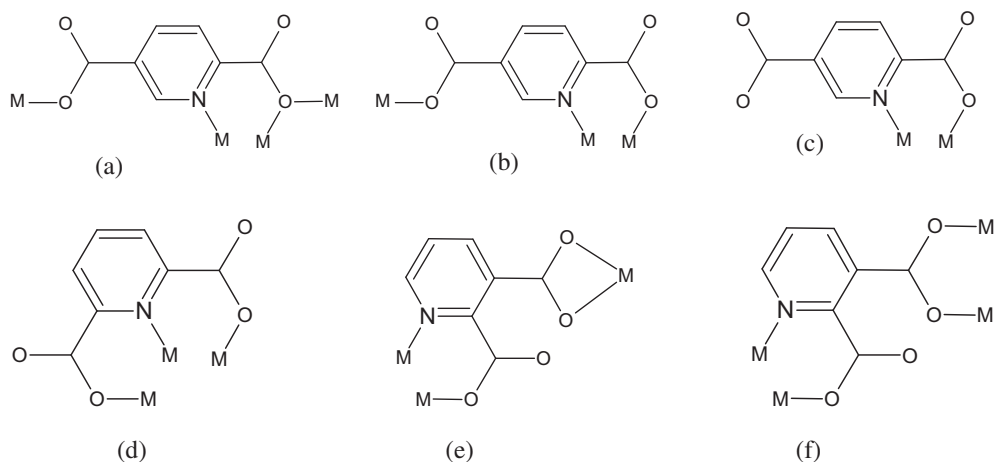
Single-crystal X-ray data were collected at room temperature with a Rigaku Saturn 724 CCD diffractometer equipped with a graphite-monochromatic Mo $K\alpha$ radiation ($\lambda = 0.71073$ Å) by using an ϕ - ω scan mode at 293(2) K. The structures were solved by direct methods with SHELXS-97 program [14] and refined by SHELXL-97 [15] using full-matrix least-squares techniques on F^2 . All non-hydrogen atoms were refined anisotropically, and the hydrogen atoms were generated theoretically onto the specific atoms and refined isotropically with fixed thermal factors. The H-atoms of water molecules have not been localized. The detailed crystallographic data and structure refinement parameters for the compounds **1–6** are summarized in Table 1. Selected bond lengths and angles are listed in Table S1 (Supplementary Data). The crystal structure representation of complexes **1–6** were made by the software DIAMOND [16].

3. Results and discussion

3.1. Structural analysis of complexes **1–6**

3.1.1. Crystal structure of $[Cd(MEDPQ)(2,5\text{-pydc})]_n$ (**1**)

Single-crystal X-ray diffraction analysis reveals that the asymmetric unit of complex **1** consists of one Cd(II) ion, one MEDPQ ligand and one 2,5-pydc anion. As shown in Fig. 1a, each Cd(II) is surrounded by a distorted octahedral geometry consisting of two



Scheme 2. Coordination modes of carboxylic groups in complexes **1–6**.

nitrogen atoms from one MEDPQ chelating ligand, one nitrogen atom from 2,5-pydc anion and three oxygen atoms belonging to three carboxyl groups from three separated 2,5-pydc anions. The Cd–O distances are longer than those found in Cd–pydc complex [17].

Both carboxyl groups present in 2,5-pydc ligands are coordinated in a monodentate mode (Scheme 2a), and bridging Cd(II) centers into a dinuclear cluster with Cd···Cd distances of 3.731 Å. The dinuclear cluster may be viewed as the basic unit, which is connected to the same four clusters by four carboxyl groups of 2,5-pydc ligands (Fig. 1b), giving rise to a layer (Fig. 1c). Considering the dinuclear cluster as nodes and keeping the 2,5-pydc ligands as spacers, we can see that the layer is composed of a four-connected

rhombic grid topology. It should be pointed out that the coordination mode of 2,5-pydc anion is very different from the related complexes $[\text{Cd}_2(\text{OH})_2(2,4\text{-pydc})]$ [17] and $[\text{Cd}(2,3\text{-pydc})(\text{H}_2\text{O})_2]_n$ [18]. Additionally, the layers are packed through weak C–H···O hydrogen bonds originating from the phen ring H9A atom of MEDPQ ligand and the coordinated carboxyl O2 atom of 2,5-pydc anion into a supramolecular network (Fig. 1d).

3.1.2. Crystal structure of $[\text{Cd}_2(\text{MOPIP})_2(2,5\text{-pydc})_2]_n$ (**2**)

When another 5,6-substituted 1,10-phen derivative MOPIP was used in the presence of 2,5-H₂pydc, complexes **2** was obtained. Complex **2** possesses a 2D polymeric network structure and is connected into a 3D network by supramolecular interactions. The

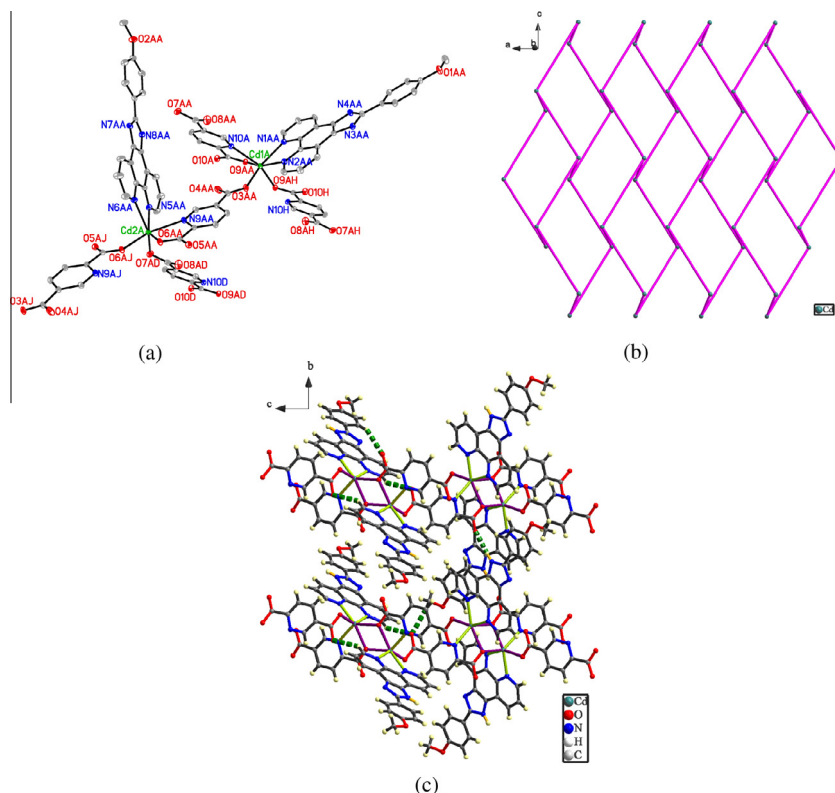


Fig. 2. (a) View of the coordination environment of Cd(II) in complex **2**; thermal ellipsoids are drawn at the 30% probability level. Hydrogen atoms have been omitted for clarity. (b) The undulating network of **2** along *ac* plan. (c) The supramolecular architecture by hydrogen bonding interactions (green broken lines represent hydrogen bonding interactions). (Color online.)

asymmetric unit of complex **2** consists of two Cd(II) ions, two MOPIP ligands and two 2,5-pydc anions. As depicted in Fig. 2a, Cd1 is hexacoordinated by two nitrogen atoms from one MOPIP chelating ligand, one nitrogen atoms from 2,5-pydc and three oxygen atoms belonging to three carboxyl groups from three separated 2,5-pydc anions. The coordination environment of Cd2 is the same as that of Cd1, as shown in Fig. 2a.

Two distorted octahedrons, which are separately formed by Cd1 and Cd2, are bridged by two μ_2 -O monodentate carboxyl groups (Scheme 2a) from two different 2,5-pydc ligands to generate a double cadmium cluster. Thus each double cadmium cluster is linked by four 2,5-pydc ligands, to lead to an undulating network along the *ac* plane (Fig. 2b). In addition, unlike **1**, the MOPIP ligands in complex **2** act as hydrogen bonding donors to the coordinated oxygen atoms of 2,5-pydc anions, and exhibits one kind of hydrogen bonding interactions (N–H...O interactions). The other kind of hydrogen bond is weak C–H...O interactions. Inter-network N–H...O and C–H...O hydrogen bonds assemble the neighboring undulating network into a supramolecular structure (Fig. 2c). In addition, the larger π -conjugated planes of MOPIP ligands generate face-to-face π ... π stacking interactions between the terminal benzene units and phen rings of MOPIP ligands in the supramolecular structure of **2** with a centroid-to-centroid distance of 3.7426(1) Å (Fig. S1). The slippage value of the terminal benzene units and phen rings is 1.1433 Å. Significant π interactions also play a significant role in the stabilization of the supramolecular structure.

3.1.3. Crystal structure of $[\text{Cu}_2(\text{MOPIP})_2(2,5\text{-pydc})_2]\cdot\text{H}_2\text{O}$ (**3**)

In order to investigate the effect of the metal centers on their complex structures, two metals Cu(II) and Mn(II) were selected to react with 2,5-H₂pydc and MOPIP under the same synthetic conditions. Two new complexes $[\text{Cu}_2(\text{MOPIP})_2(2,5\text{-pydc})_2]\cdot\text{H}_2\text{O}$ and $[\text{Mn}(\text{MOPIP})_2(2,5\text{-pydc})]\cdot 3\text{H}_2\text{O}$ were obtained. The asymmetric unit of compound **3** is shown in Fig. 3a. There are two Cu(II) ions, two MOPIP ligands, two 2,5-pydc anions and one water molecule. Cu1 lies on a general position and has a pentacoordinated square pyramidal geometry as exemplified by its tau parameter of $\tau = 0.085$ (where the τ range from 0 to 1 represents the geometric distortions from a perfect square pyramid to a trigonalbipyramid, respectively) [19]. The geometry is comprised of three nitrogen atoms from one MOPIP chelating ligand and one 2,5-pydc anion, and two oxygen atoms belonging to two carboxyl groups from two separated 2,5-pydc. Cu2 has a similar coordination environment.

Two crystallographically independent 2,5-pydc anions in the complex **3** are coordinated to two Cu(II) ions through four oxygen atoms of the carboxyl groups and two nitrogen atoms (Scheme 2b) to form a dinuclear structure. In the adjacent nuclei, face-to-face π ... π stacking interactions between the imidazole and phen ring of MOPIP ligands are found with the centroid-to-centroid separations of 3.7635(8) and 3.4823(9) Å. The slippage values of two rings are 1.897 and 0.9948 Å. The resulting discrete dinuclear structure is further cross-linked via the π ... π stacking interactions to generate a layer (Fig. S2). Moreover, the weak C–H...O hydrogen bonding

interactions are present between the adjacent dinuclear Cu units and assemble the neighboring layer into a supramolecular structure (Fig. 3b). To the best of our knowledge, this unique layer Cu cluster has not been reported so far, although other 3D Cu coordination polymer including 3,4-pydc as bridging ligands have been reported [20].

3.1.4. Crystal structure of $[\text{Mn}(\text{MOPIP})_2(2,5\text{-pydc})]\cdot 3\text{H}_2\text{O}$ (**4**)

Complex **4** exhibits a mononuclear molecule structure. The asymmetric unit of complex **4** consists of one Mn(II) ions, two MOPIP ligands, one 2,5-pydc anions and three water molecules. As depicted in Fig. 4a, each Mn(II) ion is hexacoordinated and exhibits a octahedral environment supplied by four nitrogen atoms from the MOPIP ligand, one nitrogen atom from one 2,5-pydc anion, and one oxygen atom from the same 2,5-pydc anion.

The 2,5-pydc anions in complex **4** only act as terminal ligands to connect Mn(II) ions (Scheme 2c), which result to a mononuclear structure. The centroid-to-centroid distances in the range of 3.5097(1) to 3.7244(2) Å (The slippage values are from 0.8306 to 1.4682 Å.) between a pair of MOPIP ligands in adjacent mononuclear units are observed, showing significant intra-molecular face-to-face π ... π stacking interactions. The mononuclear structure may be viewed as the basic subunit which is connected by π ... π stacking interactions, giving rise to a chain (Fig. 4b). In complex **4**, inter-chain N–H...O and C–H...O hydrogen bonds are present and assemble the neighboring chain into a supramolecular structure (Fig. S3).

3.1.5. Crystal structure of $[\text{Cd}(\text{MOPIP})_2(2,6\text{-pydc})]\cdot 3\text{H}_2\text{O}$ (**5**)

To evaluate the effect of the position of carboxyl groups on the framework formation of complex, we selected 2,6-H₂pydc and 2,3-H₂pydc to react with cadmium salt in the presence of the same MOPIP ligand. The complexes **5** and **6** with different structures, compared to complex **2**, were obtained. Complex **5** exists as a neutral mononuclear compound. The asymmetric unit of complex **5** consists of one Cd(II) ions, two MOPIP ligands, one 2,6-pydc anions and three water molecules. As depicted in Fig. 5a, Each Cd(II) center is heptacoordinated (Scheme 2d) in a distorted pentagonal bipyramidal geometry consisting of four nitrogen donors from the MOPIP ligand, one nitrogen donor from the 2,6-pydc ring and two oxygen atoms from two carboxyl groups of one 2,6-pydc ligand.

The independent mononuclear units are packing through face-to-face π ... π interactions between phen rings at a centroid-to-centroid distance of 3.7903(5) Å (The slippage value of two phen rings is 1.2078 Å.), and edge-to-face π ... π interactions between terminal benzene units at a centroid-to-face distance of 3.5955(7) Å, which result in the formation of a layer structure as presented in Fig. 5b. Significant hydrogen bonding interactions are also implicated for the reinforcement and overall stability of the crystal lattice. Complex **5** exhibits strong N–H...O, C–H...O and C–H...N hydrogen bonds between MOPIP rings and 2,6-pydc molecules (Fig. S4). PLATON analysis [21] shows that total potential solvent accessible void volume is 69.5 Å³. The percentage of the total cell volume is 1.7%.

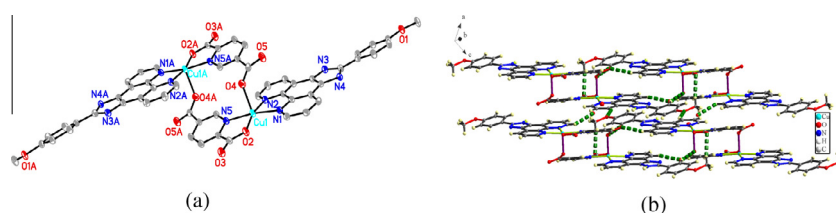


Fig. 3. (a) View of the coordination environment of Cu(II) in complex **3**; thermal ellipsoids are drawn at the 30% probability level. Hydrogen atoms have been omitted for clarity. (b) The supramolecular architecture by hydrogen bonding interactions (green broken lines represent hydrogen bonding interactions). (Color online.)

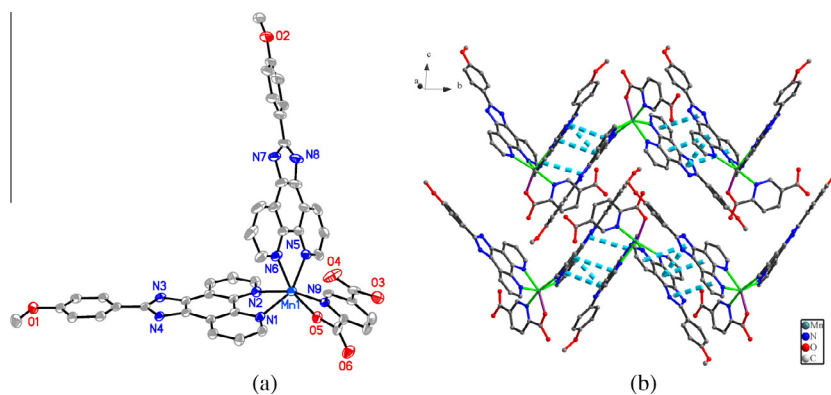


Fig. 4. (a) View of the coordination environment of Mn(II) in complex **4**; thermal ellipsoids are drawn at the 30% probability level. Hydrogen atoms have been omitted for clarity. (b) The chain structure by $\pi \cdots \pi$ stacking interactions (blue broken lines represent $\pi \cdots \pi$ stacking interactions). (Color online.)

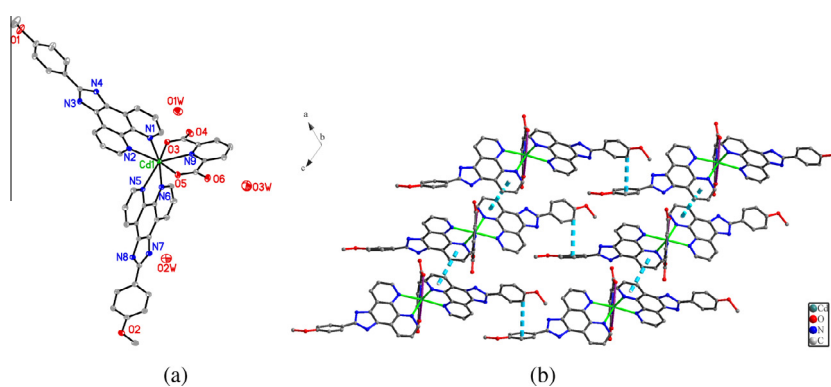


Fig. 5. (a) View of the coordination environment of Cd(II) in complex **5**; thermal ellipsoids are drawn at the 30% probability level. Hydrogen atoms have been omitted for clarity. (b) The layer structure by $\pi \cdots \pi$ stacking interactions (blue broken lines represent $\pi \cdots \pi$ stacking interactions). (Color online.)

3.1.6. Crystal structure of $[Cd_2(MOPIP)_2(2,3\text{-pydc})_2 \cdot H_2O]_n$ (**6**)

Complex **6** was crystallized in triclinic crystal system. The asymmetric unit of compound **6** consist of two Cu(II) ions, two MOPIP ligands, two 2,3-pydc anions and one coordinated water molecule. Of the two Cd(II) centers, Cd(1) is heptacoordinated by two nitrogen atoms from the MOPIP ring, one nitrogen donor from the 2,3-pydc ring, three oxygen atoms from two carboxyl groups of two different 2,3-pydc ligands and one oxygen atoms from the coordinated water molecule. It exhibited a distorted pentagonal bipyramidal geometry. The second Cd(II) ion, Cd(2), is surrounded by two nitrogen atoms from the MOPIP ring, one nitrogen donor from the 2,3-pydc ring and three oxygen atoms from two carboxyl groups of two different 2,3-pydc molecules in a distorted octahedral geometry, as depicted in Fig. 6a.

Thus, there are two crystallographically independent Cd(II) ions along with the MOPIP groups and two 2,3-pydc anions in the asymmetric unit of complex **6**. The two 2,3-pydc anions exhibit differences in their connectivity with Cd(II) ions into a infinite chain with a loop (Fig. 6b). Out of two carboxylates present in one pyridine-2,3-dicarboxylic acid, one carboxylate group is coordinated in a chelating bidentate or bridging dimonodentate mode, whereas the other is coordinated in a monodentate mode as depicted in Scheme 2e and 2f. In addition, inter-chain strong N–H \cdots O and C–H \cdots O hydrogen bonding interactions between MOPIP rings and 2,3-pydc molecules are present and assemble the neighboring chain into a layer (Fig. 6c). There exist weak face-to-face $\pi \cdots \pi$ stacking interactions (the centroid-to-face distance is 3.5971(10) Å) among phen rings of MOPIP ligands from neighboring chains, which further stabilize the layer of complex **6** (Fig. S5).

3.2. Effect of the center ions and N-donor ligands on the structures of the complexes

It is well-known that different metal centers, bearing different stereochemically active lone-pair electrons and ionic radius, can adopt variable coordination numbers and versatile coordination modes such as hemidirected and holodirected geometries. These decisive factors can be successful to construct complexes with different structures and dimensions [4b]. Two kinds of coordination numbers are observed in them: hexacoordinated for **2** and **4**, and five-coordinated for **3**. On the other hand, in complexes **2** and **4**, the coordination sphere of the central ion Cd(II) and Mn(II) is holodirected, whereas in complexes **3**, the coordination sphere of Cu(II) ion can be regarded as hemidirected and shows the presence of a stereochemically active lone pair of electrons (Fig. S6). As a result, the structural differences of **2–4** imply that the number of the coordination sites and the coordination geometry of the different center ions have an important influence on the formation of their structures. Moreover, the selection of metal centers with dissimilar coordination preferences can influence the coordination modes of the carboxylate anions and framework dimensionality of these coordination polymers. This can presumably be attributed to the metal-controlled assembly. For example, complexes **3** and **4** show a binuclear dimer and a mononuclear structure; whereas the 2,5-pydc anion has a different bridging mode, which results complex **2** shows an undulating network.

As important phen derivatives, the 5,6-substituted 1,10-phen ligands of MEDPQ and MOPIP both contain an extended π -system, an pyrazine (or imidazole) ring and additional coordination sites,

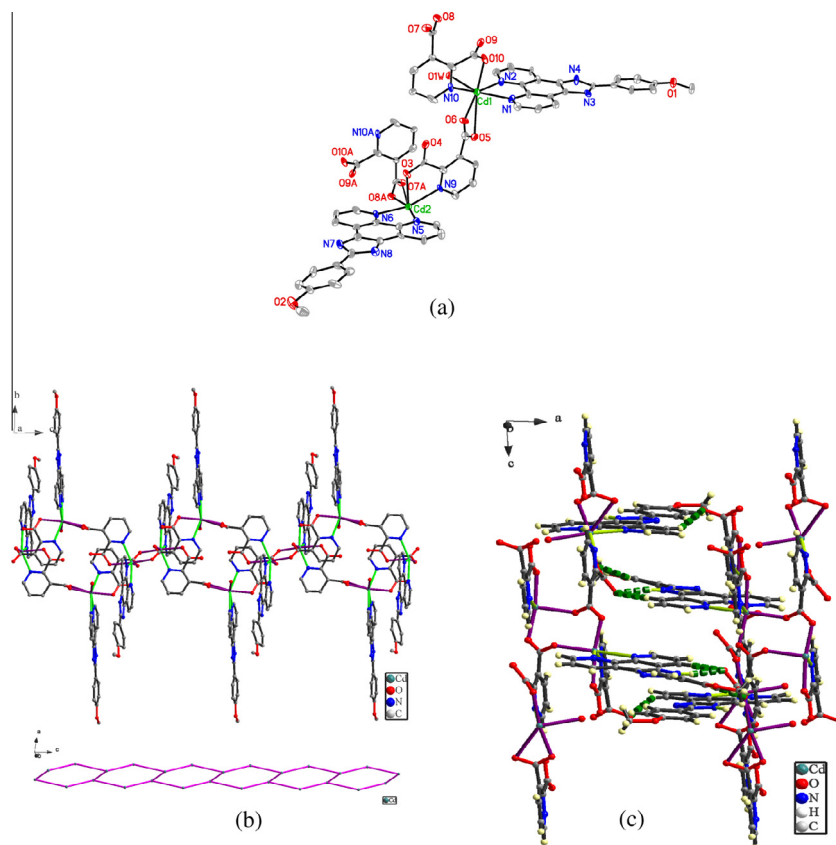


Fig. 6. (a) View of the coordination environment of Cd(II) in complex **6**; thermal ellipsoids are drawn at the 30% probability level. Hydrogen atoms have been omitted for clarity. (b) The chain with a loop of complex **6**. (c) The layer structure by hydrogen bonding interactions (green broken lines represent hydrogen bonding interactions). (Color online.)

capable of acting as hydrogen bond acceptors/donors or of forming coordination interactions to some metal ions [5d]. Obviously, the coordination behavior of MEDPQ and MOPIP ligand is similar to 1,10-phen in complexes **1–6**, which exhibits a strongly chelating coordination mode. Comparing MEDPQ and MOPIP, the differences are the imidazole ring and additional benzene ring, which may allow the MOPIP ligand have more chance to assemble higher dimensional complexes in the presence of the bigger N-donor ligand. Complex **1** shows the hydrogen bonding interactions originating from H atom of the phen ring and the O atom of carboxylate anion. It is different from MOPIP; the imidazole ring in the MOPIP ligand is a good hydrogen bonding donor. On the other hand, it is noteworthy that the $\pi \cdots \pi$ stacking interactions are found in complexes **2–6** and play the most important roles in the assembly of supramolecular structures. So, the MOPIP ligands have more important function in the formation of the supramolecular framework.

3.3. Effect of organic carboxylate anions on the structures of the complexes

According to previous reports, the role of organic carboxylate anions can be illustrated in terms of their differences in shape. Owing to the N-donor ligand with a large conjugated π -system, the selecting of multiple carboxylic acid units have proved to be good candidates because they can connect metal ions into coordination polymers exhibiting intriguing structure and dimensional diversities. In this paper, the structural differences of **2**, **5** and **6** indicate that organic carboxylate anions are also important factors in the

formation of such coordination architectures in the presence of the same MOPIP ligand and cadmium ions.

In contrast, the 2,5- H_2 pydc, 2,6- H_2 pydc and 2,3- H_2 pydc possess different steric hindrance, and the two carboxylate groups have 180, 120 and 60 °C angles, respectively. The 2,5- H_2 pydc is a very flexible ligand, and the two carboxyl groups bridge adjacent Cd_2 units into an undulating network in **2**. Different from 2,5- H_2 pydc, the carboxyl groups of 2,3- H_2 pydc adopt a chelating bidentate mode or bridging dimonodentate coordination mode, which results in a chain in **6**. When the rigid ligand 2,6- H_2 pydc was employed, a mononuclear compound **5** was obtained. Obviously, as far as complexes **2**, **5** and **6**, the distinct positions of the organic carboxyl groups result in the different coordination modes of the carboxylate ligand, which further determine the final structures of complexes.

3.4. FT-IR analysis

The FT-IR spectra of the compounds **1–6** exhibit strong characteristic absorptions for the carboxyl groups of the 2,5-pydc, 2,6-pydc and 2,3-pydc ligands in the asymmetric and symmetric vibration regions. The asymmetric stretching vibration $\nu_{as}(COO^-)$ appears in the range of 1628–1607 cm^{-1} , and 1344–1386 cm^{-1} for the symmetric stretching vibration $\nu_s(COO^-)$ [22,23]. The difference ($\Delta = 226\text{--}267\text{ }cm^{-1}$ for **1–6**) between $\nu_s(COO^-)$ and $\nu_{as}(COO^-)$ is much more than that of an ionic carboxylate unit, which indicates that carboxyl groups are monodentate coordinated with metals, which is in agreement with the crystal structure [24]. Meanwhile, The band corresponding to pyridine ring vibrations $\nu_{C=N}$ is observed at lower wave number, 1525–1521 cm^{-1} . This

negative shift with respect to the ligand indicates the coordination of pyridine nitrogen to the metal atom [25]. Weak absorptions observed at 3192–3053 cm^{-1} can be attributed to $\nu_{\text{C-H}}$ of the benzene ring. The band of 1485–1474 cm^{-1} is attributed to the skeleton vibration of the pyridine ring. The signal at 551–507 cm^{-1} for compounds **1–6** also proves the coordination of metal ions and nitrogen atoms. The band at 480–440 cm^{-1} for **1–6** indicates that the metal ions are coordinated with oxygen atoms [26]. The broad bands at around 3440–3419 cm^{-1} are attributed to the vibrations of water molecules.

3.5. Fluorescent properties

The solid-state fluorescence spectra of **2–4** at room temperature were recorded. The free MOPIP ligand also display emission with two main emission peaks at 380 and 469 nm upon excitation at 292 nm (Fig. S7), which probably be assigned to the $\pi \rightarrow \pi^*$ transitions. The complex **2** exhibits a little red shift with the bands at 382 and 471 nm ($\lambda_{\text{ex}} = 292$ nm). The red shift emission peak probably is related to the intraligand fluorescent emission, and similar red shifts have been observed before [23,27]. The emission peaks of **3** and **4** (380 and 469 nm ($\lambda_{\text{ex}} = 292$ nm)), are mainly from the MOPIP ligand. Due to the differences of their topological structures, which result to the emission bands of **2–4** is diverse. The result indicates that the fluorescence behavior is closely associated with the metal ions and the ligands coordinated around them.

3.6. Thermal properties

Thermal stability of the compounds **1** and **2** was performed by using thermogravimetric (TG) analyzer (Fig. S8). The compound **1** shows a two-step weight loss. The first weight loss of 31.39% (calcd. 31.52%) occurs from 350 to 450 °C, which corresponds to the loss of 2,5-pydc ligands. The second weight loss of 46.91% (calcd. 47.02%) between 620 and 1200 °C is ascribed to the loss of one MEDPQ ligand. For **2**, the framework begins to collapse at 330 °C, which is assigned to the release of 2,5-pydc ligands (obsd 25.93%, calcd. 27.34%), and the departure of MOPIP ligands occur from 600 to 1308 °C (obsd 50.51%, calcd. 54.04%). After the decomposition, the final product may be CdO.

3.7. NBO analysis

The selected natural atomic charges, natural electron configuration, Wiberg bond indexes and NBO bond order (a.u.) for compounds **2–4** are shown in Table S2. It can be concluded that the Cd(II) ion coordinating to O and N atoms is mainly on 5s and 4d orbitals and Cu(II) (and Mn(II)) ion is mainly on 4s and 3d orbitals (the electron number of other orbitals is so small that can be omitted) [28], O atoms and N atoms bonding with Cd(II) (Cu(II) and Mn(II)) ion are all on 2s and 2p orbitals (the electron number of 3p orbit is so small that can be omitted). Therefore, the Cd(II) (Cu(II) and Mn(II)) ion obtains some electrons from MOPIP and 2,5-pydc ligand. The differences of their bond lengths make the NBO bond orders be different [29], which is good agreement with the X-ray crystal structural data of compounds **2–4**.

Fig. S9 shows the lowest unoccupied (LUMO) and the highest occupied (HOMO) molecular orbitals of the complexes **2–4**. The LUMO orbitals are concentrated mainly in the center of the molecules. The greater contributions of the LUMO orbitals come from d orbit of the Cu(II) (and Mn(II)) ion in compound **3** and **4**, with further significant contributions from π orbitals of imidazole rings of MOPIP in compounds **2–4**. On the other hand, the HOMO levels show greater contributions of π orbitals of 2,5-pydc anion in compound **2** and **3**, and π orbitals of benzene rings and imidazole rings in MOPIP, with smaller contributions from d orbit in Mn(II) ion in compound **4**.

Such frontier orbitals characterize the ligand–ligand and ligand–metal charges transition for these kinds of compounds.

4. Conclusion

Six metal–organic coordination complexes with new topologies have been obtained under hydrothermal conditions by reactions of different 5,6-substituted 1,10-phen derivatives and transition metal salts together with organic carboxylate anion ligands. Three types of coordination structures (0D, 1D, 2D) have been observed according to the selection of metal centers with different coordination preferences, as well as the variation of the binding fashions of organic carboxylate ligands. Moreover, two 5,6-substituted 1,10-phen ligands (MEDPQ and MOPIP) with the large conjugate system play crucial roles in the formation of a supramolecular framework by $\pi \cdots \pi$ stacking and hydrogen bonding interactions.

Acknowledgement

This work is supported by the Research Fund for the Doctoral Innovative Program of Jiangsu Province (No. CXLX11_0581).

Appendix A. Supplementary data

CCDC 893357, 891047, 891045, 891098, 909209 and 909210 contains the supplementary crystallographic data for compounds **1–6**. These data can be obtained free of charge via <http://www.ccdc.cam.ac.uk/conts/retrieving.html>, or from the Cambridge Crystallographic Data Centre, 12 Union Road, Cambridge CB2 1EZ, UK; fax: +44 1223 336 033; or e-mail: deposit@ccdc.cam.ac.uk. Supplementary data associated with this article can be found, in the online version, at <http://dx.doi.org/10.1016/j.poly.2013.04.054>.

References

- [1] (a) M. Eddaoudi, J. Kim, N. Rosi, D. Vodak, J. Wachter, M. O'Keeffe, O.M. Yaghi, *Science* 295 (2002) 469; (b) J.S. Seo, D. Whang, H. Lee, S.I. Jun, J. Oh, Y.J. Jeon, K. Kim, *Nature* 404 (2000) 982.
- [2] L. Wang, W. You, W. Huang, C. Wang, X.Z. You, *Inorg. Chem.* 48 (2009) 4295.
- [3] (a) A. Schilt, *Applications of 1,10-Phenanthroline and Related Compounds*, Pergamon, London, 1969; (b) P. Tomasik, Z. Ratajczak, *Pyridine Metal Complexes*, John Wiley & Sons, New York, 1985; (c) P.G. Sammes, G. Yahioglu, *Chem. Soc. Rev.* 23 (1994) 327.
- [4] (a) G.B. Che, Z.S. Su, W.L. Li, B. Chu, M.T. Li, Z.Z. Hu, Z.Q. Zhang, *Appl. Phys. Lett.* 89 (2006) 103511; (b) G.B. Che, C.B. Liu, B. Liu, Q.W. Wang, Z.L. Xu, *CrystEngComm* 10 (2008) 184; (c) G.B. Che, J. Chen, X.C. Wang, C.B. Liu, C.J. Wang, S.T. Wang, Y.S. Yan, *Inorg. Chem. Commun.* 14 (2011) 1086; (d) X.C. Wang, C.B. Liu, J. Chen, X.Y. Li, G.B. Che, Y.S. Yan, *Z. Anorg. Allg. Chem.* 637 (2011) 698.
- [5] (a) X.L. Wang, Y.F. Bi, H.Y. Lin, G.C. Liu, *Cryst. Growth Des.* 6 (2007) 1086; (b) X.L. Wang, Y.F. Bi, G.C. Liu, H.Y. Lin, T.L. Hu, X.H. Bu, *CrystEngComm* 10 (2008) 349; (c) G.C. Liu, Y.Q. Chen, X.L. Wang, B.K. Chen, H.Y. Lin, *J. Solid State Chem.* 182 (2009) 566; (d) X.L. Wang, Y.Q. Chen, Q. Gao, H.Y. Lin, G.C. Liu, J.X. Zhang, A.X. Tian, *Cryst. Growth Des.* 10 (2010) 2174; (e) X.L. Wang, Y.Q. Chen, G.C. Liu, H.Y. Lin, W.Y. Zheng, J.X. Zhang, *J. Organomet. Chem.* 694 (2009) 2263.
- [6] (a) M.D. Stephenson, M.J. Hardie, *Cryst. Growth Des.* 6 (2006) 423; (b) M.D. Stephenson, T.J. Prior, M.J. Hardie, *Cryst. Growth Des.* 8 (2008) 643.
- [7] (a) C.V. Sastri, D. Eswaramoorthy, L. Giribabu, B.G. Maiya, *J. Inorg. Biochem.* 94 (2003) 138; (b) A. Ambrose, B.G. Maiya, *Inorg. Chem.* 39 (2000) 4264.
- [8] Z.H. Weng, D.C. Liu, Z.L. Chen, H.H. Zou, S.N. Qin, F.P. Liang, *Cryst. Growth Des.* 9 (2009) 4163.
- [9] A.C. Wibowo, M.D. Smith, *Cryst. Growth Des.* 11 (2011) 4449; (b) Y.S. Song, B. Yan, L.H. Weng, *Inorg. Chem. Commun.* 9 (2006) 567; (c) X.C. Wang, C.B. Liu, X.Y. Li, C.X. Li, Y.S. Yan, G.B. Che, *Chin. J. Inorg. Chem.* 26 (2010) 2126; (d) R. Mishra, M. Ahmad, M.R. Thipathi, *Polyhedron* 50 (2013) 22.
- [10] M.L. Hu, Y.P. Lu, H.M. Zhang, B. Tu, Z.M. Jin, *Inorg. Chem. Commun.* 9 (2006) 962.

- [11] (a) M.N. Manjunatha, A.G. Dikundwar, K.R. Nagasundara, *Polyhedron* 30 (2011) 1299;
(b) K.J. Wei, Y.S. Xie, J. Ni, M. Zhang, Q.L. Liu, *Cryst. Growth Des.* 6 (2006) 1341.
- [12] (a) Y.J. Huang, Y.C. Cui, G. Du, J. *Inorg. Chem.* 25 (2009) 1882;
(b) B. Liu, S. Zhou, X.M. Li, C.B. Li, *Chin. J. Struct. Chem.* 27 (2008) 1195;
(c) L. Wang, L. Ni, J. *Coord. Chem.* 65 (2012) 1475;
(d) L. Wang, L. Ni, J. Yao, *Solid State Sci.* 14 (2012) 1361.
- [13] M.J. Frisch, G.W. Trucks, H.B. Schlegel, *GAUSSIAN 03 Revision B. 03*, Gaussian, Inc., Pittsburgh PA, 2003.
- [14] G.M. Sheldrick, *SHELXS-97*, Program for Solution of Crystal Structures, University of Göttingen, Germany, 1997.
- [15] G.M. Sheldrick, *SHELXL-97*, Program for Refinement of Crystal Structures, University of Göttingen, Germany, 1997.
- [16] W.T. Pennington, *J. Appl. Cryst.* 32 (1999) 1028.
- [17] M.L. Tong, S. Hu, J. Wang, S. Kitagawa, S.W. Ng, *Cryst. Growth Des.* 5 (2005) 837.
- [18] M. Li, J.F. Xiang, L.J. Yuan, S.M. Wu, S.P. Chen, J.T. Sun, *Cryst. Growth Des.* 6 (2006) 2036.
- [19] A.W. Addison, T.N. Rao, J. Reedijk, J. Van Rijn, G.C. Verschoor, *J. Chem. Soc., Dalton Trans.* (1984) 1349.
- [20] M.L. Tong, J. Wang, S. Hu, S.R. Batten, *Inorg. Chem. Commun.* 8 (2005) 48.
- [21] A.L. Spek, *PLATON*, The University of Utrecht, Utrecht, The Netherlands, 1999.
- [22] X.J. Zhang, Y.H. Xing, Z. Sun, J. Han, Y.H. Zhang, M.F. Ge, S.Y. Niu, *Cryst. Growth Des.* 7 (2007) 2041.
- [23] C.C. Wang, Z.H. Wang, F.B. Gu, G.S. Guo, *J. Mol. Struct.* 1004 (2011) 39.
- [24] X. Shi, G.S. Zhu, X.H. Wang, G.H. Li, Q.R. Fang, X.J. Zhao, G. Wu, G. Tian, M. Xue, *Cryst. Growth Des.* 5 (2005) 341.
- [25] S. Prasanna, B.R. Bijini, K. Rajendra Babu, S.M. Eapen, M. Deepa, C.M.K. Nair, *J. Cryst. Growth* 333 (2011) 36.
- [26] K. Nakamoto, *Infrared and Raman Spectra of Inorganic and Coordination Compounds*, fourth ed., Wiley Interscience, New York, 1986.
- [27] X. Shi, G. Zhu, Q. Fang, G. Wu, G. Tian, R. Wang, D. Zhang, M. Xue, S. Qiu, *Eur. J. Inorg. Chem.* (2004) 185.
- [28] X. Peng, G.H. Cui, D.J. Li, T.F. Liu, *J. Mol. Struct.* 967 (2010) 54.
- [29] Z.P. Li, Y.H. Xing, Y.H. Zhang, *Acta Phys. Chim. Sin.* 25 (2009) 741.